INSTITUTE OF PHYSICS PUBLISHING JOURNAL OF PHYSICS B: ATOMIC, MOLECULAR AND OPTICAL PHYSICS

J. Phys. B: At. Mol. Opt. Phys. **37** (2004) 1841–1857 PII: S0953-4075(04)70455-1

Experimental investigation of electron and positron interactions with monosubstituted and disubstituted benzene derivatives: fluorobenzene, 1, 3-difluorobenzene and 1, 4-difluorobenzene molecules

C Makochekanwa, O Sueoka and M Kimura

Graduate School of Science and Engineering, Yamaguchi University, Ube, Yamaguchi 755-8611, Japan

Received 2 October 2003, in final form 5 March 2004
Published 20 April 2004
Online at stacks.iop.org/JPhysB/37/1841 (DOI: 10.1088/0953-4075/37/9/006)

Abstract

Electron and positron scattering from fluorobenzene (C_6H_5F), 1, 3-difluorobenzene (1, 3-$C_6H_4F_2$) and 1, 4-difluorobenzene (1, 4-$C_6H_4F_2$) molecules have been investigated experimentally using the linear transmission time-of-flight method. Total cross sections (TCSs) were measured and determined for 0.8–600 eV and 0.7–600 eV, respectively, for electron and positron scattering from 1, 3-$C_6H_4F_2$ and 1, 4-$C_6H_4F_2$ molecules, and 0.4–1000 eV and 0.2–1000 eV, respectively, for electron and positron scattering from C_6H_5F molecules. A broad resonance structure has been observed in the C_6H_5F electron TCSs at 0.8–1.6 eV, corresponding to the 1.6 eV $^2E_{2u}$ C_6H_6 resonance structure. This broad structure seems to be made of two structures at 0.8 eV and 1.4 eV, which should mean that the original single 1.6 eV resonance peak in the C_6H_6 parent molecule has split into two upon the monosubstitution of its H atom by the F atom. 1, 3-$C_6H_4F_2$ electron TCSs show a rising trend below 2 eV, a feature attributed to the polar nature of these molecules. Above 4 eV for all these three molecules, electron TCSs are greater than positron TCSs by a factor of ∼2 at energies up to 40 eV.

1. Introduction

Aromatic molecules such as benzene molecules and their derivatives are some of the most fundamental organic molecules which are the building blocks leading to further rich biochemical and material science. Therefore, spectroscopic and dynamical knowledge of these molecules is essential for various applications. We have recently conducted comparative studies on electron and positron scattering from benzene and its benzene derivatives [1, 2] in order to shed more light on the underlying physics of interaction schemes of electron and

 © 2004 IOP Publishing Ltd Printed in the UK

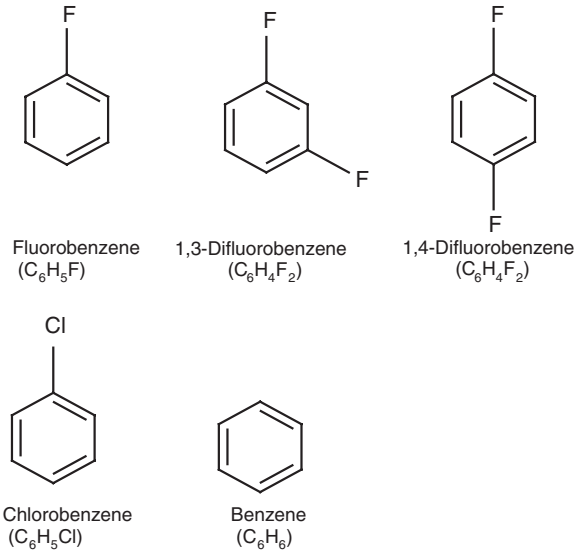

Figure 1. Molecular diagrams for all molecules.

positron with a molecule and to provide a set of total cross-section (TCS) data in a wide range of collision energy from a tenth of an eV to a keV. Furthermore, we have identified a few new resonance-like structures in electron scattering, and observed oppositely rise and fall trends in benzene TCSs below 0.5 eV for electron and positron impacts that are caused by the difference in interaction potentials for electron and positron.

There has been a long history of electron interaction investigation on these molecules based on various experimental techniques. For low-energy electron scattering, transmission experiments range from investigations of the lowest negative ion resonances for fluorobenzenes [3–5], the compound negative-ion resonances and threshold electron-excitation states for monosubstituted benzene derivatives [6, 7] and mobilities of thermal electrons in some of these π-electron containing benzene derivatives [8]. Investigations of the correlations between the ionization potentials and basicities in aromatic carbonyl compounds [9] and the effect, on electron affinities, of substituting atoms/radicals into these molecules [10], have also been carried out. No report on the systematic cross-section measurement for these molecules, however, has been published. Though some limited studies on integral and backward scattering, by Lunt *et al* [11], for C_6H_5F molecules were attempted, absolutely no study on $1,3\text{-}C_6H_4F_2$ and $1,4\text{-}C_6H_4F_2$ molecules exists.

Neither theoretical nor experimental investigations on positron scattering exist for any of these molecules so that the present results are the first comprehensive studies to be reported.

In this paper, comparative studies of total scattering processes by electron and positron impacts for fluorobenzene (C_6H_5F), 1,3-difluorobenzene ($1,3\text{-}C_6H_4F_2$) and 1,4-difluorobenzene ($1,4\text{-}C_6H_4F_2$), are presented. See figure 1 for molecular diagrams and table 1 for some useful molecular properties that exist in the literature [11, 12].

The impact energies are from 0.8–600 eV and 0.7–600 eV, respectively, for electron and positron scattering from $1,3\text{-}C_6H_4F_2$ and $1,4\text{-}C_6H_4F_2$ molecules, and 0.4–1000 eV and 0.2–1000 eV, respectively, for electron and positron scattering from C_6H_5F molecules. The results are compared with those of the parent benzene (C_6H_6) molecule for better understanding of the substitutional effects. Firstly, electron TCSs for all molecules are analysed together,

Table 1. Molecular properties.

Molecule	Dipole moment[a] (Debye)	Polarizability[a] (au)	Ionization potential[a] (eV)	Asymmetry parameter[b] (κ)	Molecular diameter[c] (Å)
C_6H_5F	1.60	69.5	9.200	−0.5877	7.21
C_6H_5Cl	1.69	95.2	9.06	−0.8497	7.69
$1,3\text{-}C_6H_4F_2$	1.51	69.5	9.33		7.31
$1,4\text{-}C_6H_4F_2$	–	66.1	9.14		7.52
C_6H_6	–	69.4	9.2459		6.91

[a] After Lide [12].
[b] After Lunt *et al* [11].
[c] After Harte [20].

in comparison with those of C_6H_6, for group patterns in their scattering properties. Here the effects of monosubstitution (C_6H_5F, C_6H_5Cl) and disubstitution ($1,3\text{-}C_6H_4F_2$, $1,4\text{-}C_6H_5F_2$) of the F atoms into the C_6H_6 ring structure on the scattering dynamics are studied. Secondly, TCSs for electron scattering from C_6H_5F are studied in comparison with those from C_6H_5Cl and C_6H_6. Special attention is given here to examining the effect, on the scattering physics, of the difference in the monosubstituting atom, i.e. substitution of the H atom by the F atom between C_6H_5F and C_6H_6 on one hand, and substitution of the H atom by the Cl atom between C_6H_5Cl and C_6H_6 on the other hand. Thirdly, the disubstituted molecules are discussed. Our interest in this study is to understand the difference of the effect, on the scattering, that results from *meta*-disubstitution ($1,3\text{-}C_6H_4F_2$) compared to *para*-disubstitution ($1,4\text{-}C_6H_5F_2$) of the two H atoms into the C_6H_6 ring structure. Next, positron scattering from these molecules is analysed using the same style as the foregoing electron impact part. Lastly, electron and positron scattering are studied for the individual molecules in the order C_6H_5F, $1,3\text{-}C_6H_4F_2$ and $1,4\text{-}C_6H_5F_2$. A brief discussion is also provided on the electron and positron scattering of C_6H_5F compared with those of C_6H_5Cl, from our previous work [1], since both of these molecules are monosubstituted halobenzenes.

2. Experimental method

The absolute TCSs for electron and positron scattering from these molecules have been measured using the linear transmission retarding potential time-of-flight (RP-TOF) method in an apparatus set-up similar to our previous measurements [13], and only briefly explained here. An $\sim$80 μCi ^{22}Na radioactive source produces fast positrons, which are converted to a slow beam using an annealed seven-overlapping-layer mesh tungsten moderator set baked at 2100 °C. The energy width of the positron beam was about 2.2 eV. For electron scattering, the slow electrons are produced as secondary electrons emerging from the moderator surfaces after multiple scattering. The electron beam had an energy spread of about 1.4 eV. A pair of Helmholtz coils is used for the cancelling of the effect of the magnetic field due to the Earth in the region of the collision cell.

The TCS values, Q_t, are derived from the Beer–Lambert relation applied as

$$Q_t = -\frac{1}{nl} \ln \frac{I_g}{I_v} \tag{1}$$

where I_g and I_v refer to the projectile beam intensities transmitted through the collision cell with and without the target gas of number density n, respectively; l refers to the effective length

of the collision cell and was established by normalizing our measured positron–N_2 TCSs to those of the positron–N_2 data of Hoffman *et al* [14]. This measurement serves not only as a normalization procedure in the measurement of the effective length, but also for checking the pressure gauge stability. It neither changed significantly for electron nor positron TCS measurements. As Kennerly and Bonham [15] pointed out earlier, this pressure gauge stability check and the pressure independence of the TCSs highlighted below are an important aspect of measurements using a collision cell in the transmission RP-TOF set-up.

A magnetic field parallel to the flight path, due to the solenoid coils, is applied for beam transportation. The entrance and exit apertures of the collision cell are very wide, being 3 mm in radius. Accordingly, the measured raw TCS data are to some extent affected by forward scattering effects and a correction for this forward scattering effect is usually necessary. This correction depends not only on the geometrical conditions, including the magnetic field, but also on the differential cross section (DCS) data. Unfortunately, because no DCS data are available for all these three molecules, the data presented here could not be corrected for these forward scattering effects. As a result, it is thus possible that the TCSs presented here may be a few per cent smaller in magnitude.

Nevertheless, we have learnt from our experience with the correction for other molecules that the correction, if carried out, could have possibly resulted in TCSs that are larger than the ones presented here by a few per cent but with no effect on the positions and type of structures observed in our data, so that these data should be credible and useful for application. However, this conjecture on the effect of the forward scattering correction will not hold for molecules, whose DCSs are a subtle function of energy.

Specific experiments for TCS independence of gas pressure were omitted for these molecules for economic reasons. However, because all our other measurements with the same apparatus up to now [16], and other molecules on these 'benzene-related' series investigated over the same period [1, 2], have all shown the measured TCS to be independent of gas pressure, we infer the same here.

2.1. Errors in the measurements

The errors in the results presented in tables 2–4 are the total uncertainties. These total uncertainties were computed from the equation

$$\frac{\Delta Q_t}{Q_t} = \frac{\Delta n}{n} + \frac{\Delta l}{l} + \frac{\Delta I}{I}. \tag{2}$$

This sum of all the uncertainties for electron scattering was estimated to be 5.5–7.4% for C_6H_5F, 5.7–8.4% for 1,3-$C_6H_4F_2$ and 5.7–6.6% for 1,4-$C_6H_4F_2$ molecules. The same sum of intensities for positron scattering was 6.5–12.7% for C_6H_5F, 6.5–8.7% for 1,3-$C_6H_4F_2$ and 7.0–9.6% for 1,4-$C_6H_4F_2$ molecules. These sums of uncertainties are made up of contributions from the beam intensities, $\Delta I/I$, where I refers to $\ln(I_g/I_v)$ in equation (1), which were <2.4% (<7.7%) for C_6H_5F, <3.4% (3.5%) for 1,3-$C_6H_4F_2$ and <2.1% (4.7%) for 1,4-$C_6H_4F_2$ molecules for electron (positron) scattering. The contribution from the gas density was <3% for all target gas molecules and for both projectiles, while that due to the determination of the effective length of the collision cell, $\Delta l/l$, was about 2% for both projectiles and all molecules.

3. Results and discussion

Electron and positron scatterings are separately discussed below. A simplified approach was used to estimate the magnitudes of the increases in TCSs due to the forward scattering,

Table 2. Fluorobenzene (C_6H_5F) TCSs (10^{-16} cm^2) for electron and positron scattering.

Energy (eV)	Electron	Positron	Energy (eV)	Electron	Positron
0.2		23.7 ± 3.0	11	51.6 ± 2.9	27.0 ± 2.0
0.4	33.3 ± 2.4	25.1 ± 2.7	12	50.6 ± 2.8	28.1 ± 2.1
0.6	37.0 ± 2.3	28.9 ± 2.8	13	48.3 ± 2.6	30.3 ± 2.3
0.8	40.5 ± 3.0	32.6 ± 2.9	14	46.7 ± 2.6	28.6 ± 2.3
1.0	39.9 ± 2.3	33.1 ± 2.7	15	44.7 ± 2.5	25.4 ± 2.1
1.2	40.2 ± 2.3		16	44.0 ± 2.5	26.3 ± 2.2
1.3		32.3 ± 2.6	17	42.5 ± 2.4	26.1 ± 2.1
1.4	40.7 ± 2.3		18	41.7 ± 2.5	25.9 ± 2.0
1.6	39.8 ± 2.3	31.6 ± 2.5	19	42.3 ± 2.5	26.5 ± 2.1
1.8	39.6 ± 2.4		20	41.4 ± 2.6	26.7 ± 2.2
1.9		33.5 ± 2.5	22	39.9 ± 2.3	29.2 ± 2.0
2.0	38.2 ± 2.3		25	36.7 ± 2.1	29.3 ± 2.2
2.2	37.4 ± 2.1	33.4 ± 2.5	30	34.8 ± 2.1	27.6 ± 2.1
2.5	36.2 ± 2.1	35.5 ± 2.6	35	32.6 ± 2.0	
2.8	36.5 ± 2.1	36.8 ± 2.7	40	32.3 ± 1.9	27.0 ± 1.9
3.1	36.4 ± 2.2	38.6 ± 2.9	50	31.0 ± 1.8	27.0 ± 1.8
3.4	37.5 ± 2.2	33.5 ± 2.7	60	32.0 ± 1.8	26.2 ± 1.7
3.7	38.7 ± 2.3	34.5 ± 2.7	70	27.1 ± 1.6	24.2 ± 1.6
4.0	38.4 ± 2.2	35.3 ± 2.6	80	25.4 ± 1.4	23.8 ± 1.7
4.5	41.7 ± 2.4	34.4 ± 2.5	90	26.3 ± 1.6	22.9 ± 1.7
5.0	43.0 ± 2.5	33.0 ± 2.4	100	24.7 ± 1.5	22.8 ± 1.7
5.5	44.1 ± 2.5	33.9 ± 2.4	120	21.3 ± 1.3	20.6 ± 1.5
6.0	44.0 ± 2.5	32.7 ± 2.4	150	21.0 ± 1.2	19.5 ± 1.4
6.5	44.9 ± 2.6	36.7 ± 2.7	200	17.9 ± 1.1	18.5 ± 1.3
7.0	44.5 ± 2.5	33.8 ± 2.4	250	17.0 ± 1.0	15.4 ± 1.2
7.5	47.9 ± 2.7	32.8 ± 3.2	300	14.8 ± 0.8	13.0 ± 1.0
8.0	49.1 ± 2.8	34.0 ± 2.4	400	12.9 ± 0.7	12.0 ± 0.9
8.5	51.2 ± 2.9	31.3 ± 2.3	500	11.1 ± 0.6	10.0 ± 0.8
9.0	51.1 ± 2.9	28.3 ± 2.1	600	9.46 ± 0.5	8.76 ± 0.7
9.5	50.5 ± 2.9	26.9 ± 2.0	800	6.99 ± 0.4	7.94 ± 0.6
10	49.7 ± 2.8	27.0 ± 1.9	1000	6.02 ± 0.3	6.98 ± 0.6

especially for the electron data where the effect of the dipole moments in C_6H_5F (1.60 D) and $1,3$-$C_6H_4F_2$ (1.51 D) is expected to be non-negligible at low energies below a few eV. By way of studying the increases due to this forward scattering observed in our systematic study of methyl halides [17], where the data for CH_3F were deduced by regression analysis, the relationship between the percentage increases in the data for CH_4 (non-polar) and CH_3F (polar) electron TCSs was mimicked to infer on the relationship between the corresponding data for C_6H_6 (non-polar) and C_6H_5F (polar) below 5 eV. The results show that the forward scattering correction carried on C_6H_5F could result in increases of about 14%, 11%, 10%, 12%, 16% and 17% at 0.8, 1.0, 1.6, 2.0, 3.1 and 5.0 eV, respectively, compared to C_6H_6 whose increments at the same energies were calculated to be 2.1%, 1.7%, 1.6%, 1.9%, 2.4% and 2.5%. Neglecting other factors and only arguing on the influence of the dipole moment, then not so different (from C_6H_5F) increment rates would be expected also in the data for $1,3$-$C_6H_4F_2$ because of its near equal dipole moment magnitude. No data at hand can aid in giving a clue to what the increments can be expected to be for $1,4$-$C_6H_4F_2$ non-polar molecules, though these would be expected to be at least more than in C_6H_6. This correction carried out for positron TCSs would result in increases typically up to 20% greater than the electron case [2].

Table 3. 1, 3-difluorobenzene (1, 3-$C_6H_4F_2$) TCSs (10^{-16} cm^2) for electron and positron scattering.

Energy (eV)	Electron	Positron	Energy (eV)	Electron	Positron
0.7		19.2 ± 1.6	12	45.4 ± 2.8	31.3 ± 2.1
0.8	47.1 ± 3.9		13	44.3 ± 2.8	32.4 ± 2.2
1.0	43.2 ± 2.7	22.1 ± 1.8	14	44.2 ± 2.7	31.0 ± 2.1
1.2	43.9 ± 2.7		15	42.9 ± 2.7	30.2 ± 2.1
1.3		23.7 ± 2.0	16	43.9 ± 2.6	31.5 ± 2.2
1.4	42.5 ± 2.6		17	43.4 ± 2.7	32.0 ± 2.3
1.6	41.8 ± 2.6	28.9 ± 2.2	18	42.5 ± 2.7	32.3 ± 2.2
1.8	40.0 ± 2.5		19	42.6 ± 2.9	31.6 ± 2.2
1.9		32.3 ± 2.2	20	41.9 ± 2.6	30.9 ± 2.1
2.0	39.1 ± 2.6		22	41.0 ± 2.5	30.5 ± 2.0
2.2	38.1 ± 2.3	33.5 ± 2.2	25	39.2 ± 2.6	31.7 ± 2.1
2.5	38.8 ± 2.4	31.3 ± 2.1	30	37.4 ± 2.8	30.2 ± 1.9
2.8	37.8 ± 2.4	32.1 ± 2.2	35	35.6 ± 2.3	
3.1	37.9 ± 2.6	31.4 ± 2.2	40	37.5 ± 2.2	29.9 ± 1.9
3.4	39.6 ± 2.4	32.4 ± 2.2	50	35.4 ± 2.2	28.4 ± 1.8
3.7	40.3 ± 2.5	32.3 ± 2.1	60	32.9 ± 2.1	27.3 ± 1.8
4.0	40.0 ± 2.4	32.6 ± 2.0	70	30.1 ± 1.8	27.0 ± 1.8
4.5	47.3 ± 2.7	31.0 ± 2.0	80	29.6 ± 1.8	26.0 ± 1.7
5.0	46.3 ± 2.8	31.9 ± 2.1	90	28.4 ± 1.7	25.4 ± 1.7
5.5	44.7 ± 2.6	31.6 ± 2.1	100	25.8 ± 1.6	24.4 ± 1.6
6.0	44.7 ± 2.7	32.6 ± 2.2	120	25.2 ± 1.5	24.3 ± 1.6
6.5	45.3 ± 2.7	32.6 ± 2.2	150	22.2 ± 1.4	21.7 ± 1.5
7.0	46.9 ± 2.8	33.3 ± 2.2	200	19.6 ± 1.2	19.9 ± 1.4
7.5	47.8 ± 2.8	31.9 ± 2.2	250	17.2 ± 1.0	18.0 ± 1.2
8.0	47.0 ± 2.9	31.6 ± 2.2	300	16.8 ± 1.0	16.1 ± 1.2
8.5	47.4 ± 2.9	31.0 ± 2.3	400	14.0 ± 0.8	14.3 ± 1.0
9.0	49.6 ± 3.0	31.6 ± 2.3	500	11.9 ± 0.7	12.5 ± 0.9
9.5	48.8 ± 2.9	30.8 ± 2.2	600	11.4 ± 0.7	11.3 ± 0.8
10	47.7 ± 2.8	30.8 ± 2.1			
11	45.8 ± 2.8	31.8 ± 2.0			

A detailed comparison with the C_6H_6 molecule for each molecule, as well as with C_6H_5Cl for C_6H_5F, is attempted for better understanding of the characteristics of the observed structures. Numerical values for these TCSs are displayed in tables 2–4.

3.1. Electron scattering

Electron TCSs for all three molecules, C_6H_5F, 1, 3-$C_6H_4F_2$ and 1, 4-$C_6H_4F_2$, are shown in figure 2, together with those of C_6H_5Cl and C_6H_6 from our earlier studies [1, 2]. Except for the low-energy region below 6 eV, all four TCS curves, including C_6H_5Cl, show energy dependence patterns that strongly resemble those of the C_6H_6 case, regardless of the number of substitutions of the H atoms in the C_6H_6 that take place, i.e. regardless of monosubstitution such as in C_6H_5F and C_6H_5Cl, or disubstitution such as in 1, 3-$C_6H_4F_2$ and 1, 4-$C_6H_4F_2$. As apparent, the change in structure of the C_6H_6 ring resulting from the substitutional effects surely affects more the scattering dynamics in the low-energy region than the higher energy of a few tens of eV because of the longer interaction time with the incident particle. The $^2E_{2u}$ resonance for C_6H_6 observed at 1.6 eV [2] is also seen in these molecules, but shifts to somewhat lower energies, i.e. at 1.0 eV or below.

Table 4. 1, 4-difluorobenzene (1, 4-$C_6H_4F_2$) TCSs (10^{-16} cm^2) for electron and positron scattering.

Energy (eV)	Electron	Positron	Energy (eV)	Electron	Positron
0.7		38.3 ± 3.7	13	50.8 ± 3.2	31.2 ± 2.3
0.8	39.6 ± 2.3		14	48.5 ± 3.0	30.5 ± 2.2
1.0	40.4 ± 2.3	31.7 ± 2.7	15	49.2 ± 3.0	30.8 ± 2.2
1.2	41.4 ± 2.4		16	48.0 ± 2.9	31.6 ± 2.2
1.3		32.8 ± 2.7	17	48.4 ± 2.9	30.6 ± 2.2
1.4	42.0 ± 2.5		18	47.5 ± 2.9	30.6 ± 2.2
1.6	42.6 ± 2.6	32.7 ± 2.7	19	47.5 ± 3.0	30.4 ± 2.2
1.8	41.7 ± 2.5		20	46.8 ± 2.9	29.6 ± 2.3
1.9		30.8 ± 2.6	22	44.9 ± 2.7	28.7 ± 2.1
2.0	40.1 ± 2.4		25	43.7 ± 2.6	29.6 ± 2.2
2.2	38.3 ± 2.3	32.0 ± 2.4	30	42.7 ± 2.5	29.5 ± 2.0
2.5	39.2 ± 2.3	32.0 ± 2.4	35	42.2 ± 2.5	
2.8	38.7 ± 2.3	31.5 ± 2.4	40	40.1 ± 2.3	27.1 ± 1.9
3.1	38.5 ± 2.4	33.2 ± 2.4	50	38.5 ± 2.2	26.5 ± 1.9
3.4	39.7 ± 2.5	31.7 ± 2.5	60	36.4 ± 2.0	26.7 ± 1.9
3.7	40.6 ± 2.6	32.1 ± 2.5	70	35.0 ± 2.0	25.8 ± 1.9
4.0	41.9 ± 2.6	32.3 ± 2.3	80	33.6 ± 2.0	24.4 ± 1.8
4.5	45.0 ± 2.7	34.4 ± 2.4	90	31.6 ± 1.9	24.8 ± 1.8
5.0	45.8 ± 2.8	32.4 ± 2.6	100	30.0 ± 1.8	24.0 ± 1.8
5.5	45.9 ± 2.8	33.1 ± 2.4	120	27.6 ± 1.6	21.4 ± 1.6
6.0	46.9 ± 2.9	32.4 ± 2.4	150	24.6 ± 1.5	20.4 ± 1.6
6.5	48.4 ± 2.9	32.3 ± 2.3	200	21.9 ± 1.3	18.1 ± 1.5
7.0	49.9 ± 3.0	31.3 ± 2.3	250	18.9 ± 1.1	17.2 ± 1.3
7.5	50.1 ± 3.1	31.7 ± 2.3	300	18.0 ± 1.1	15.4 ± 1.2
8.0	52.0 ± 3.2	31.9 ± 2.3	400	15.1 ± 1.0	12.9 ± 1.1
8.5	51.6 ± 3.3	32.1 ± 2.3	500	12.9 ± 0.8	11.4 ± 1.0
9.0	53.4 ± 3.5	32.1 ± 2.3	600	12.0 ± 0.7	10.3 ± 0.9
9.5	54.4 ± 3.4	30.6 ± 2.2			
10	53.7 ± 3.2	30.2 ± 2.1			
11	52.6 ± 3.2	31.0 ± 2.2			
12	52.1 ± 3.1	30.5 ± 2.3			

It is also worth mentioning here that C_6H_5F and 1, 3-$C_6H_4F_2$ are polar molecules and have large polarizabilities, while the 1, 4-$C_6H_4F_2$ molecule is non-polar, but has a relatively large polarizability with the value of 66.1 au (table 1). As a result, their low-energy electron scattering cross sections are expected to be dominated by these dipole, or polarization effects, in which the richness in structure of all the TCSs below about 6 eV is apparent. Briefly, in this energy region, the interaction time of the electron with the molecule is sufficiently long hence causing large deformations in the electron cloud of the molecule, and the change of the molecular field may cause a change in scattering potential resulting in a shape resonance. This shape resonance should then be responsible for the structures seen in this region. However, joint theoretical and experimental investigations are surely needed for complete elucidation and assignment of each of these structures.

All molecules show the strong shape-resonance peak at about 9 eV. At this peak energy, the order of magnitude of the cross section is $C_6H_5Cl > 1, 4\text{-}C_6H_4F_2 > (C_6H_5F \approx 1, 3\text{-}C_6H_4F_2)$. This trend roughly reflects the molecular size. Beyond this peak, say above 50 eV, all TCSs fall off gradually, and the magnitude of the TCSs becomes exactly proportional to the molecular size in which the additive rule may provide a reasonable interpretation. TCSs for all molecules,

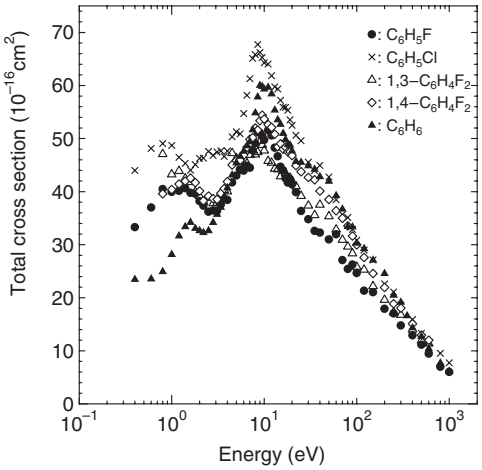

Figure 2. Electron TCSs for (●) C_6H_5F, (×) C_6H_5Cl, (△) 1, 3-$C_6H_4F_2$, (◇) 1, 4-$C_6H_4F_2$ and (▲) C_6H_6 molecules.

C_6H_5F, C_6H_5Cl and 1, 3- and 1, 4-$C_6H_4F_2$ clearly show a characteristic structure, possibly due to direct impact ionization, centred at about 50 eV, that is exactly identical to that observed in C_6H_6.

3.1.1. C_6H_5F. As discussed in our study of C_6H_5Cl, the substitution of an atom or radical destroys the symmetry of the benzene ring, and thus the degenerate e_{2u} orbital of the benzene molecule splits into two [1]. This splitting is explained by the fact that low-lying unoccupied orbitals of benzenes are anti-bonding π orbitals, written as $\pi_4{}^*$, $\pi_5{}^*$ and $\pi_6{}^*$, with the first pair ($\pi_4{}^*$, $\pi_5{}^*$) in the parent C_6H_6 molecule degenerate. In the case of a monosubstitution, one member of this pair will be symmetric (*S*) and the other antisymmetric (*A*). It has been studied that only one of these $\pi^*(S)$ can interact in a resonance fashion with the substituent atomic orbitals of p_z symmetry [4]. Monosubstitution on C_6H_6 leads to migration of the charge between the foreign atom (F in this case) and the C_6H_6 ring with the result that the degeneracy is lifted. Apart from this splitting, Mathur and Hasted's [7] transmission spectra of the C_6H_6 derivatives are seen to be largely uniform and resemble that of the C_6H_6 molecules in the general features, despite large changes in symmetry.

The TCSs for C_6H_5F, shown in figure 3 together with those of C_6H_5Cl and C_6H_6, have several structures, which are somewhat stronger than others, that are analysed as follows.

Low-energy range below 8 eV. (i) The TCSs drop rather rapidly below 0.8 eV, like those of C_6H_5Cl and C_6H_6 molecules. However, because C_6H_5F, like C_6H_5Cl, molecules have a dipole moment, eventually they are expected to rise instead at much lower energies, because the presence of a dipole moment makes the molecule an effective scattering centre, as energy decreases below a few eV, resulting in increased rotationally inelastic scattering events. This behaviour, however, is still not seen in our current low-energy range down to 0.4 eV. (ii) Oltholff *et al* [4], in their electron transmission studies, observed the splitting of the C_6H_6 ($\pi_4{}^*$, $\pi_5{}^*$) degenerate pair due to the resonant interaction between the symmetrical member of this pair and the substituent's occupied F2p_z orbital. This split shows up as resonant structures at 0.87 and 1.48 eV in their results. Our results, however, do not show this effect in the form of two clearly resolved structures but shows only a broad single-resonance peak extending

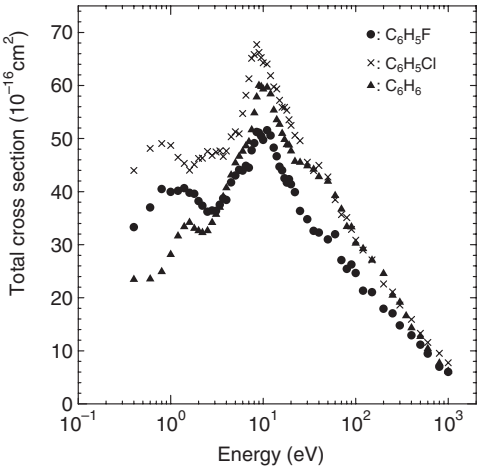

Figure 3. Electron TCSs for (●) C_6H_5F, (×) C_6H_5Cl and (▲) C_6H_6 molecules.

from 0.8 to 1.6 eV, though with unpronounced shoulders at 0.8 and 1.4 eV. These resonance features may have cross-section values that are too small to be seen in the TCSs, that have magnitudes of the order of 40×10^{-16} cm^2 in this energy region. These features correspond to the single $^2E_{2u}$ resonance for C_6H_6 observed at 1.6 eV [2]. The result for C_6H_5Cl, however, clearly shows the splitting of this 1.6 eV C_6H_6 resonance peak in the form of two peaks, one at 0.8 eV and another one centred at about 2.5 eV. As for C_6H_5F, the dissociative electron attachment (DEA) channel is also expected to enhance TCSs at energies around 1 eV and above [11, 18]. However, as Lunt *et al* [11] observed, cross sections due to DEA are small with a value of the order <1 Å^2, and therefore DEA does not play a significant role in the interpretation of our TCSs here. (iii) These C_6H_5F TCSs show a minimum at 2.5 eV that corresponds to that in C_6H_6 at 2.2 eV. (iv) Below this minimum, the order of the cross-section magnitude is $C_6H_5Cl > C_6H_5F > C_6H_6$, i.e. proportional to the molecular size. (v) Above this minimum, the TCSs gradually increase towards the main peak, which is at 8–11 eV. (vi) It is worth noting too, though, that these TCSs show an unresolved shoulder at about 5 eV. The origin of such a structure has not been extensively examined, though it is interesting to note that C_6H_6 TCSs show a similar feature, at about 4.5 eV, which has been attributed to the $^2B_{2g}$ resonance studied by Cho *et al* [19], in their studies they determined its energy to be 4.94 eV.

Energy region above 8 eV. (i) These TCSs show the main resonance peak in the same energy region of 8–11 eV like both C_6H_6 and C_6H_5Cl. (ii) At this peak the magnitude of the TCSs appears to be in the order $C_6H_5Cl > (C_6H_6) > C_6H_5F$. The order of the last two species is somewhat puzzling in view of the molecular size, but TCSs for C_6H_6 were found to be larger than those of C_6F_6 [1]. Hence the present result is, at least, consistent with our earlier C_6H_6 and C_6F_6 measurements. (iii) This peak, for C_6H_5F, should be made up of two structures at 8.5 eV and 11 eV as described above. These structures are, however, overshadowed by the error bars, though still visible. (iv) At energies above this peak, whereas TCSs for C_6H_5Cl and C_6H_6 show some characteristic shoulder, possibly due to impact ionization centred at about 45 eV, that in C_6H_5F TCSs is found to be somewhat weaker. (v) C_6H_5F TCSs are lower than the other two at all energies above the main peak. However, they seem to be approaching C_6H_6 TCSs at energies above 600 eV.

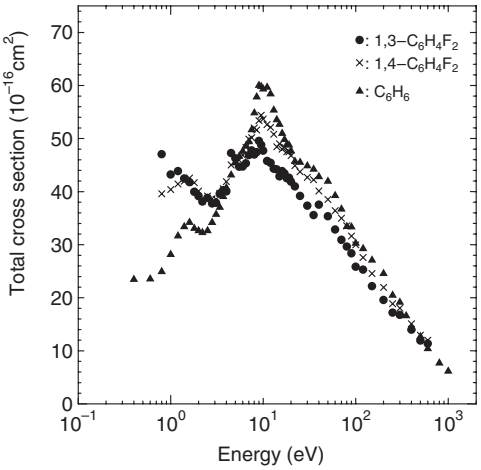

Figure 4. Electron TCSs for (●) 1, 3-$C_6H_4F_2$, (×) 1, 4-$C_6H_4F_2$ and (▲) C_6H_6 molecules.

3.1.2. 1, 3-$C_6H_4F_2$ and 1, 4-$C_6H_4F_2$. Although the 1, 4-disubstitution of F atoms in C_6H_6 is expected to be more symmetrical than the above C_6H_5F monosubstitution case, owing to the molecular structures, 1, 3-disubstitution does not help the symmetry in the resultant benzene derivative either (see figure 1). Nevertheless, even in the disubstitution, the splitting of the degenerate e_{2u} orbital in the C_6H_6 parent molecule is still expected, i.e. similar to the split resonance states studied by Christophorou *et al* [6] and Mathur and Hasted [7] for some benzene derivatives. This is because irrespective of the nature of substitution, i.e. mono- or di-substitution, and added to this, regardless of the location of substitution, for example, whether 1, 4- or 1, 3-disubstitution, resonance and inductive effects are solely governed by the change of the electron distribution within a molecule. Here resonance is associated with migration of electrons from the substituent atom X to the benzene ring B, and the inductive properties determine the extent of electron migration from B to X. For both molecules, the chemistry of the F substituent means that it draws electrons from the benzene ring, resulting in resonance processes.

The results for these two molecules are shown in figure 4, together with those for C_6H_6 molecules. The observed structures are analysed as follows. Except for 1, 3-$C_6H_4F_2$ molecules, which show a continually rising trend in TCSs below 2 eV, the TCSs for these two molecules have structures that resemble those of the C_6H_6 parent molecule. From rough inspection of these TCS curves, 1, 4-$C_6H_4F_2$ TCSs clearly show the best resemblance to the C_6H_6 TCSs. This is not surprising since a 1, 4-disubstitution is more symmetrical than a 1, 3-disubstitution (see figure 1). That 1, 3-$C_6H_4F_2$ TCSs continue to rise below 2 eV is expected for these molecules because of the strong dipole moment (1.51 D) [12] resulting in increased rotationally inelastic scattering at such energies. 1, 4-$C_6H_4F_2$ TCSs show a peak at 1.6 eV. This peak corresponds to the $^2E_{2u}$ resonance for C_6H_6 observed at exactly the same energy, 1.6 eV. In these 1, 4-$C_6H_4F_2$ TCSs, however, only a single broad 1.6 eV peak is seen which may mask an envelope of the splitting. Oltholff *et al* [4], however, resolved the two energies for the (π_4^*, π_5^*) degenerate pair splitting and found them to be 0.65 eV and 1.38 eV in their electron transmission experiments. Below this 1.6 eV peak, 1, 4-$C_6H_4F_2$ TCSs show a gradual decrease whereas those of C_6H_6 show a rather rapid fall before almost levelling off below 0.8 eV. Above 3 eV, both 1, 3-$C_6H_4F_2$ and 1, 4-$C_6H_4F_2$ TCSs are seen increasing with almost the same slope as C_6H_6 TCSs. Both these TCSs reproduce the weak feature at about 4.5 eV, which is seen in

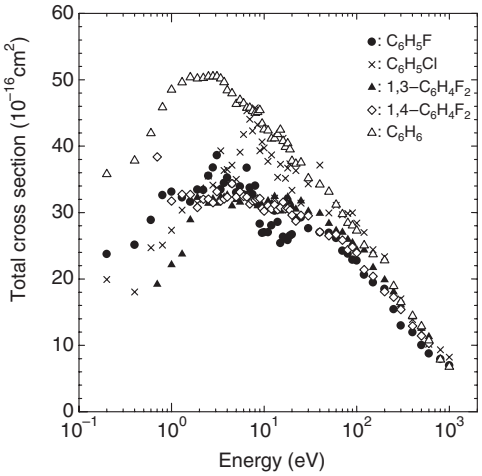

Figure 5. Positron TCSs for (●) C_6H_5F, (×) C_6H_5Cl, (▲) 1, 3-$C_6H_4F_2$, (◇) 1, 4-$C_6H_4F_2$ and (△) C_6H_6 molecules.

C_6H_6 where it has been attributed to the $^2B_{2g}$ resonance. All three TCSs rise to produce the main peak at about 9 eV. At this peak energy, the magnitude of TCSs of 1, 3-$C_6H_4F_2$ is greater than those of 1, 4-$C_6H_4F_2$. At energies above this peak, both TCSs show decreasing trends with almost the same slope. It is worth mentioning though that the characteristic shouldering at about 45 eV that was observed in the monosubstitution case of C_6H_5Cl is also seen in the TCSs for these two molecules. However, this feature is more pronounced in 1, 4-$C_6H_4F_2$ than in 1, 3-$C_6H_4F_2$ TCSs. Such a feature at these energies should possibly be due to impact ionization. Otherwise, TCSs continue to decrease above 60 eV all the way up to 1000 eV.

3.2. Positron scattering

The TCS results for positron scattering for all three molecules, C_6H_5F, 1, 3-$C_6H_4F_2$ and 1, 4-$C_6H_4F_2$, are shown in figure 5, together with those of C_6H_5Cl and C_6H_6, from our previous work [1, 2]. Except for the rising behaviour of 1, 4-$C_6H_4F_2$ TCSs below 1.5 eV, both monosubstituted (C_6H_5F, C_6H_5Cl) and disubstituted (1, 3-$C_6H_4F_2$, 1, 4-$C_6H_4F_2$) TCSs show similar general shapes as those of C_6H_6. Like C_6H_6, TCSs for C_6H_5F, C_6H_5Cl and 1, 3-$C_6H_4F_2$ decrease below 1.5 eV with almost the same slope as C_6H_6. Above this energy all TCSs show broad peaks, which are almost smooth and structureless for C_6H_6 and the disubstituted 1, 3-$C_6H_4F_2$ and 1, 4-$C_6H_4F_2$ molecules, but show structures for the monosubstituted molecules C_6H_5F and C_6H_5Cl. All TCSs decrease at energies above this peak region with almost the same slope as C_6H_6 TCSs. One possible factor that influences the behaviour of TCSs is the molecular size. When hydrogen atoms are replaced by F or Cl atoms, the molecules become larger in geometrical size and accordingly, the electron charge distribution is likely to spread out spatially increasing scattering events. Using the Corey–Pauling–Koltun (CPK) model [20], the diameters of these molecules were estimated to be in the order C_6H_5Cl > 1, 4-$C_6H_4F_2$ > 1, 3-$C_6H_4F_2$ > C_6H_5F > C_6H_6, see table 1. Thus, as a general rule, it can be said that the larger the substituting atom becomes, the larger the TCS tends to be. This could explain the greater TCSs for C_6H_5Cl compared to C_6H_5F, 1, 3-$C_6H_4F_2$ and 1, 4-$C_6H_4F_2$, above 3.5 eV, the order of magnitude of TCSs for these four molecules above 9.0 eV and the near equal TCSs for 1, 3-$C_6H_4F_2$ and 1, 4-$C_6H_4F_2$ at all energies above 2.0 eV. At energies below a few eV, however,

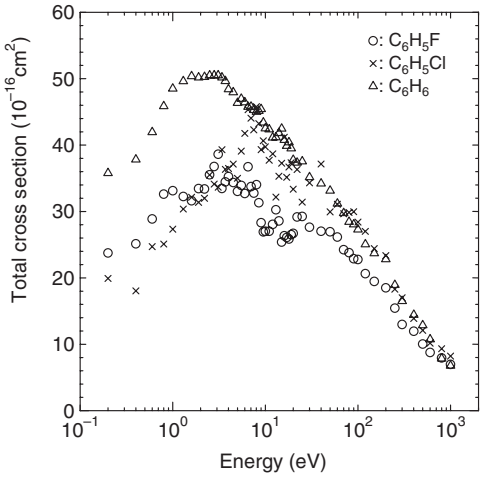

Figure 6. Positron TCSs for (○) C_6H_5F, (×) C_6H_5Cl and (△) C_6H_6 molecules.

effects of the dipole moment are expected to influence the TCS behaviour, to a greater extent also, as described above in electron scattering, which may be mostly ascribed to rotationally inelastic scattering, resulting in increasing TCSs at low energies. The magnitude of TCSs is found to be in the order of C_6H_6 (non-polar) > 1,4-$C_6H_4F_2$ (non-polar) > C_6H_5F (1.60 D) > C_6H_5Cl (1.69 D) > 1,3-$C_6H_4F_2$ (1.51 D) at energies below 2 eV, when the opposite would have been expected. At this energy, the tail part of the dominant peak at around 10 eV governs the order of the magnitude of TCSs, and hence, the order appears to be reversed. It is also worth noting that monosubstitution by the F atom (as in C_6H_5F) or Cl atom (as in C_6H_5Cl) results in TCSs that are richer in structure at low to intermediate energies than disubstitution by F atoms (as in 1,3-$C_6H_4F_2$ and 1,4-$C_6H_4F_2$). This richness in structure observed in C_6H_5F and C_6H_5Cl could also be in part due to the fact that these halobenzenes are asymmetric top molecules with asymmetry parameter values of −0.5877 and −0.8497 (see table 1), respectively, for C_6H_5F and C_6H_5Cl, which should show itself in increased rotationally inelastic-scattering and/or vibrational-excitation effects at these low to intermediate energies.

3.2.1. C_6H_5F. The positron TCSs for C_6H_5F are shown in figure 6, together with C_6H_6 and C_6H_5Cl TCSs for comparison. As highlighted above, TCSs for the parent C_6H_6 molecule show a broad and smooth peak whereas those for C_6H_5F, as well as C_6H_5Cl, show some structures that are not negligible. All three TCSs decrease below 1 eV. As pointed out above, however, this behaviour of TCSs below 1 eV is not expected because C_6H_5F (and also C_6H_5Cl) are polar molecules, and thus instead expected to have rising TCSs at such energies. The reason for this is as already highlighted above that the presence of a dipole moment enhances scattering processes, resulting in increased rotationally inelastic scattering events. It is possible though that our lowest energy of 0.2 eV could still be too high for this trend of rising TCSs to be seen.

These C_6H_5F TCSs show a weak peak centred around 1 eV, another one at about 2.1 eV and a few others at energies above 2.5 eV, before showing a continually decreasing trend above 25 eV. The origin of these peaks is not yet clear, but may well be in part due to low-lying electronic excitation arising from F atom bound and vibrational excitations, or the enhancement from some types of resonance including positron attachment, although more careful joint experimental and theoretical study on this is needed for concrete understanding. As for the

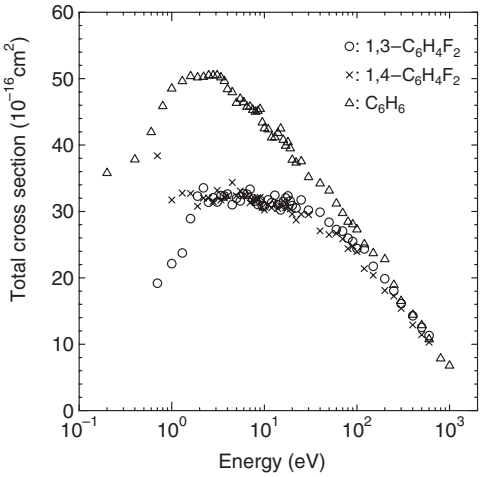

Figure 7. Positron TCSs for (○) 1, 3-$C_6H_4F_2$, (×) 1, 4-$C_6H_4F_2$ and (△) C_6H_6 molecules.

origin of the 1 eV and 2.1 eV peaks, certainly the contribution from the positronium formation channel with a threshold of 2.4 eV can be excluded from these peak structures. The ionization channel opens up with a threshold of 9.2 eV, so that it also practically does not contribute to all these structures below 9 eV. It is also intriguing that the opening up of this ionization channel is followed by falling TCSs, producing the minimum centred at 10 eV, when it would otherwise be expected to result in enhanced TCSs. Another minimum is also observed centred at 18 eV. The origin of this minimum is a combination of rise and fall of contributions from different channels.

3.2.2. 1,3-$C_6H_4F_2$ and 1,4-$C_6H_4F_2$. These TCSs are shown in figure 7, together with those of C_6H_6 for comparison.

As highlighted above, at energies below 1.5 eV, 1, 3-$C_6H_4F_2$ TCSs are instead expected to be seen rising because these molecules are polar, and the opposite to be true for C_6H_6 and 1, 4-$C_6H_4F_2$, both of which are non-polar molecules. 1, 3-$C_6H_4F_2$ and 1, 4-$C_6H_4F_2$ TCSs show broad peaks which are of almost the same width, same magnitude and broader than the C_6H_6 peak. However, C_6H_6 TCSs are more than 50% greater than both TCSs in this peak region of about 1.5–20 eV. Even at all energies above this peak, the magnitudes of these two TCSs remain within 4% of each other. These nearly identical positron TCSs for 1, 3-$C_6H_4F_2$ and 1, 4-$C_6H_4F_2$ are in contrast with the electron case, seen and discussed above, where the difference is quite significant over all collision energies, except at 2.8–5 eV. This surely suggests that, in the collision dynamics, the positron does not 'see' that much of a difference between 1, 3-$C_6H_4F_2$ and 1, 4-$C_6H_4F_2$ molecules, i.e. even though the molecular structures for these two molecules are significantly different, for this collision energy domain, and the interaction between the positron and the electron charge cloud around each of these molecules is sufficiently close for the difference to stand out clearly for the incoming positron. This is simply because the positron cannot approach sufficiently close to, or inside, the electron charge cloud because of the static interaction, hence being repelled farther out from a target without seeing much structural difference of the target. The electron case studied above is, however, different which should suggest that the electron actually 'feels' the difference between these two molecules resulting in different scattering dynamics as evidenced by the different TCSs.

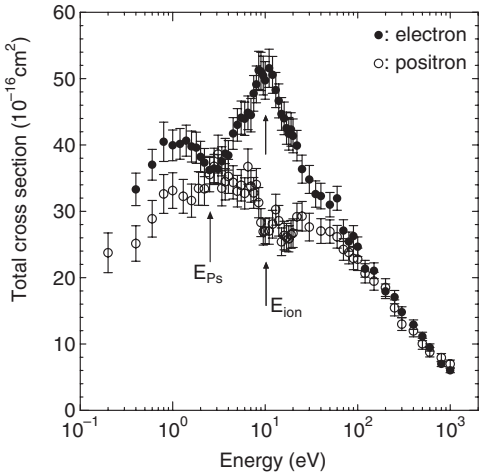

Figure 8. Electron (●) and positron (○) TCSs for C_6H_5F molecules. The error bars show total uncertainties determined as explained in the text. The arrows show the thresholds for positronium formation (E_{Ps}) and ionization (E_{ion}).

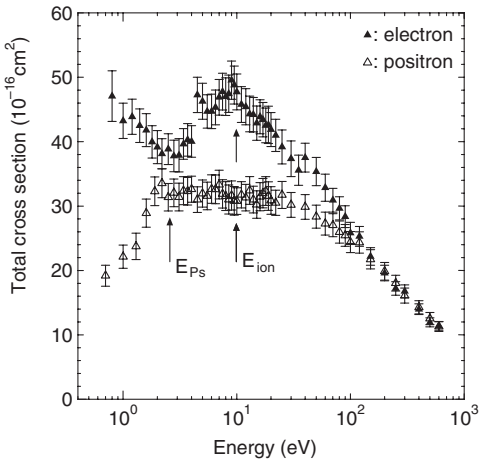

Figure 9. Electron (●) and positron (○) TCSs for 1, 3-$C_6H_4F_2$ molecules. The error bars show total uncertainties determined as explained in the text. The arrows show the thresholds for positronium formation (E_{Ps}) and ionization (E_{ion}).

3.3. A comparison of TCSs between electron and positron scattering

The electron and positron TCSs are shown in figures 8, 9 and 10 for C_6H_5F, 1, 3-$C_6H_4F_2$ and 1, 4-$C_6H_4F_2$ molecules, respectively. Some interesting features in these TCSs for each molecule are analysed as follows. Though all these three molecules are structurally different from each other as apparent from figure 1, some similarities are seen in their electron and positron TCSs.

3.3.1. C_6H_5F. At energies below 2 eV, both electron and positron TCSs show a peak around 1 eV, as described above, and decrease with roughly the same slope below this energy. However, electron TCSs are about 20% greater than their positron counterparts, which points

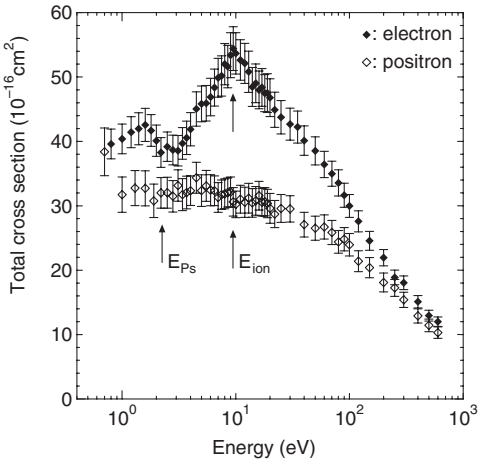

Figure 10. Electron (●) and positron (○) TCSs for 1, 4-$C_6H_4F_2$ molecules. The error bars show total uncertainties determined as explained in the text. The arrows show the thresholds for positronium formation (E_{Ps}) and ionization (E_{ion}).

to some difference in the nature of the forces at play in electron scattering from positron scattering. At energies 4–40 eV, electron TCSs show a rising trend compared to positron TCSs that are slowly decreasing. The difference between these electron and positron TCSs continues to increase until they reach the main peak at about 10 eV. At this peak, attributable to a shape resonance of the incoming electron, electron TCSs are greater than the corresponding positron TCSs by about 84%. At energies above 40 eV, however, TCSs for electron and positron slowly begin to approach each other, and tend to merge beyond a few hundred eV, as has been observed in some of our previous studies [21].

3.3.2. 1,3-$C_6H_4F_2$. At energies below 2 eV, electron and positron TCSs are found to show opposite trends, i.e. a rising trend for electron impact but a decreasing trend for positron impact. Although both TCSs are expected to rise at low energies due to the strong dipole moments, in most of our experiments [19, 21] only the TCSs for electron impact show behaviour characteristic of polar molecules in this energy range. This clearly suggests that the different interaction schemes between electron and positron impacts more significantly and sensitively contributes to the scattering dynamics in this energy range. At 4–40 eV, electron TCSs are seen rising compared to positron TCSs that are fairly constant at the peak plateau. The difference between these electron and positron TCSs continues to increase until the electron main peak at about 8 eV. Because of the dominant contribution from a shape resonance at this peak, electron TCSs are greater than the corresponding positron TCSs by about 55%. These electron and positron TCSs tend to merge above 100 eV, i.e. a slightly higher energy than that of the C_6H_5F case investigated above.

3.3.3. 1,4-$C_6H_4F_2$. Electron TCSs are found to decrease gradually below 2 eV, while positron TCSs are still on the peak plateau, or beginning to rise, as suggested by the single point at 0.7 eV. These positron TCSs are also expected to decrease similar to the electron case because of the non-polar nature of these molecules. Like the C_6H_5F case, these molecules show rising electron TCSs, compared to positron TCSs that are slowly decreasing. Again, like the other two cases above, the difference between these electron and positron TCSs continues to

increase until the main peak of the electron TCSs is reached at about 9 eV, with electron TCSs becoming greater than the positron counterparts by about 78%. Beyond this peak region, both TCSs decrease, but do not clearly show merging even at the highest energy studied at 600 eV. This is a clear difference from the previous two cases of C_6H_5F and $1,3\text{-}C_6H_4F_2$ molecules above.

That at 4–40 eV, electron TCSs are substantially greater than positron TCSs for all these molecules is a clear reflection of the differences in the interaction between the electron and positron with molecules, whereby the existence of shape resonance and attachment phenomena in electron scattering results in increased structure and enhancement of TCSs compared to positron scattering. The observation that the general trend for all these three molecules begins to merge beyond a few hundred eV should be because at these higher energies, only the first Born term dominates the scattering event. Here, the cross section varies with the square of the charge of an incoming particle, and hence, the effect of the charge difference on the cross section vanishes leading to this convergence phenomenon in the TCSs. For slower merging, this suggests that the contributions from higher order terms in the Born series are still dominant with significant effect from the exchange interaction, thus making the electron TCSs larger than positron TCSs. But when and in what case they begin to merge may well depend on the molecular shape, hence, the interaction scheme. This knowledge is still missing.

4. Conclusion

In this paper TCS data for electron and positron scattering from fluorobenzene (C_6H_5F), 1,3-difluorobenzene ($1,3\text{-}C_6H_4F_2$) and 1,4-difluorobenzene ($1,4\text{-}C_6H_4F_2$) molecules are presented. A broad resonance structure has been observed in the C_6H_5F electron TCSs at 0.8–1.6 eV, corresponding to the 1.6 eV $^2E_{2u}$ C_6H_6 resonance structure. This broad structure seems to be made of two structures at 0.8 eV and 1.4 eV, which should mean that the original single 1.6 eV $^2E_{2u}$ resonance structure in the C_6H_6 parent molecule gets split upon the monosubstitution of its H atom by the F atom. $1,3\text{-}C_6H_4F_2$ electron TCSs show a rising trend below 2 eV, a feature attributed to the polar nature of these molecules. For all these three molecules, electron TCSs are greater than positron TCSs by a factor of 1–2 at energies from above 4 eV up to 40 eV. In the comparative studies of TCSs for these molecules with C_6H_6, $1,4\text{-}C_6H_4F_2$, especially electron TCSs have shown the best resemblance to C_6H_6. This should be due to fact that the 1,4-disubstitution, using the same F atom, is more symmetrical with respect to the original C_6H_6 ring than the other two. In a result somewhat striking, TCSs for C_6H_6 have been observed to be greater than all others, except for C_6H_5Cl, at energies above 7 eV for electron and below 50 eV for positron impact. This result deviates from trends that we have observed, with a few exceptions, amongst TCSs for various molecular families studied in our laboratory, whereby TCS magnitudes have been seen to increase with increasing geometrical molecular sizes. This was explained from the simple viewpoint that when molecules become larger in geometrical size, accordingly, the electron charge distribution is likely to spread out spatially increasing scattering events, and hence resulting in larger TCSs. Electron and positron TCSs tend to merge with each other above 40 eV for C_6H_5F, above 100 eV for $1,3\text{-}C_6H_4F_2$ but are only expected above 600 eV for $1,4\text{-}C_6H_4F_2$ molecules. This observation should be because, at these higher energies, only the first Born term dominates the scattering event so that the TCS becomes independent of the charge sign on the projectile. For slower merging, this is suggestive that the contributions from higher order terms in the Born series still play a crucial role for dynamics making electron scattering larger than positron scattering. But as to when and in what case they begin to merge may well depend on the molecular shape, and hence, the interaction scheme.

Acknowledgments

This work was supported in part by a grant-in-aid from the Ministry of Education, Science, Sport, Culture and Technology, the Japan Society for Promotion of Science and a cooperative research grant from the National Institute for Fusion Science, Japan.

References

[1] Makochekanwa C, Sueoka O and Kimura M 2003 *J. Chem. Phys.* **119** 12257
[2] Makochekanwa C, Sueoka O and Kimura M 2003 *Phys. Rev.* A **68** 032707
[3] Frazier J R, Christophorou L G, Canter J G and Schweinler H C 1978 *J. Chem. Phys.* **69** 3807
[4] Olthoff J K, Tossel J A and Moore J H 1985 *J. Chem. Phys.* **83** 5627
[5] Christophorou L G, Grant M W and McCorkle D L 1977 *Adv. Chem. Phys.* **36** 413
[6] Christophorou L G, McCorkle D L and Carter J G 1974 *J. Chem. Phys.* **60** 3779
[7] Mathur D and Hasted J B 1976 *J. Phys. B: At. Mol. Phys.* **9** L31
[8] Christophorou L G, Blaunstein R P and Pittman D 1973 *Chem. Phys. Lett.* **22** 41
[9] Gal J-F, Geribaldi S, Pfister-Guillouzo G and Morris D G 1985 *J. Chem. Soc. Perkin Trans.* **2** 103
[10] Wentworth W E, Kao L W and Becker R S 1975 *J. Phys. Chem.* **79** 1161
[11] Lunt S L, Field D, Hoffmann S V, Gulley R J and Ziesel J-P 1999 *J. Phys. B: At. Mol. Opt. Phys.* **32** 2707
[12] Lide D R (ed) 2000 *CRC Handbook of Chemistry and Physics* 81st edn (Boca Raton, FL: CRC Press)
[13] Sueoka O and Mori S 1986 *J. Phys. B: At. Mol. Phys.* **19** 4035
[14] Hoffman K R, Dababneh M S, Hsieh Y-F, Kauppila W E, Pol V, Smart J H and Stein T S 1982 *Phys. Rev.* A **25** 1393
[15] Kennerly R E and Bonham R A 1978 *Phys. Rev.* A **17** 1844
[16] Sueoka O, Makochekanwa C and Kawate H 2002 *Nucl. Instrum. Methods* B **192** 206
[17] Milhaud J 1985 *Chem. Phys. Lett.* **118** 167
[18] Cho H, Gulley R J, Sunohara K, Kitajima M, Uhlmann L J, Tanaka H and Buckman S J 2001 *J. Phys. B: At. Mol. Opt. Phys.* **34** 1019
[19] Kimura M, Sueoka O, Makochekanwa C, Kawate H and Kawada M 2001 *J. Chem. Phys.* **115** 7442
[20] Harte R A 1981 *Molecules in Three Dimensions: A Guide to the Construction of Models of Biologically Interesting Compounds with CPK Models* 3rd edn (Bethesda, MD: American Society of Biological Chemists)
[21] Kimura M, Sueoka O, Hamada A and Itikawa Y 1999 *Adv. Chem. Phys.* **111** 537